UNITED STATES
DEPARTMENT OF THE INTERIOR
GEOLOGICAL SURVEY

[Reports - Open file series] 79-1621.

A PRELIMINARY STUDY OF THE COYOTE LAKE EARTHQUAKE OF AUGUST 6, 1979 AND ITS MAJOR AFTERSHOCKS

by

W.H.K. Lee, D.G. Herd, V. Cagnetti, W.H. Bakun, and A. Rapport

1979

A PRELIMINARY STUDY OF THE COYOTE LAKE EARTHQUAKE OF AUGUST 6, 1979 AND ITS MAJOR AFTERSHOCKS

by

W. H. K. Lee*, D. G. Herd*, V. Cagnetti**, W. H. Bakun*, and A. Rapport*

OPEN-FILE REPORT 79-1621

This report is preliminary and has not been edited or reviewed for conformity with Geological Survey standards and nomenclature

October, 1979

* U.S. Geological Survey, Menlo Park, CA

** C.N.E.N. Site Engineering Laboratory, Rome, Italy

ABSTRACT

The August 6, 1979 earthquake (magnitude 5.7 $\pm$ 0.2) was located about 1 km east of the Calaveras fault trace near Coyote Lake, at a depth of about 10 km. The spatial distribution of the aftershocks in the first 15 days and the focal mechanism of the main shock and selected aftershocks suggest that faulting took place primarily to the southeast of the main shock along a 25-km segment of the Calaveras fault zone at a depth of 4 to 12 km. The motion was right-lateral strike-slip along a nearly vertical fault plane. Discontinuous surface rupture was observed along a 14.4-km length of the recently active trace of the fault southeast of Coyote Lake, but no surface faulting was seen in the epicentral area. A maximum 5-mm fault offset was recorded near San Felipe Lake, about 16 km south of the main shock.

There was no prominent foreshock activity. The cumulative number of aftershocks (N) versus magnitude (M) could be described by the equation $\log N = 3.33 - 0.75\ M$, in the magnitude range between 1 and 3.5. The number and size of aftershocks appeared to be much less than that expected for a main shock of magnitude 5.7.

INTRODUCTION

A moderate-size earthquake (magnitude about 5.7) occurred near Coyote Lake at 17:05 on August 6, 1979 (GCT) approximately 10 km NNE of Gilroy, California. It caused minor damage in Gilroy, Hollister, and nearby communities, and was the largest event in this area since the magnitude 6.6 earthquake in 1911 (Richter, 1958, p. 469). This earthquake is of particular interest in that it occurred within the dense networks of geophysical instrumentation operated by the U.S. Geological Survey in central California. In this report, we summarize the results of our early investigations of the Coyote Lake earthquake and its major aftershocks which occurred in the first 15 days. Our intent is to provide timely information for others in studying these earthquakes. Due to time limitation, this study is of necessity limited in scope and is preliminary in nature.

After we completed our preliminary studies, we received a draft copy of "Observations of the Coyote Lake, California earthquake sequence of August 6, 1979" by Uhrhammer (1979) in which the main shock and 30 aftershocks were studied using primarily seismograms recorded at the University of California, Berkeley.

TECTONIC SETTING

The August 6, 1979 earthquake near Gilroy, California, was instrumentally located near the Calaveras fault zone at Coyote Lake (Fig. 1). A northwest-trending right-slip zone, the Calaveras is one of the principal recently active faults in the San Francisco Bay region. The Calaveras and its southern continuation, the Paicines fault zone, are part of a line of right-slip fault zones that branches northeastward from the San Andreas fault zone south of Hollister (Herd, 1978). More than 170 km in length, the Calaveras-Paicines fault zone extends northward through Hollister almost to Suisun Bay northeast of Oakland. Just east of San Jose the Hayward fault zone splays westward from the Calaveras. North of Hollister the Sargent fault zone cuts diagonally between the Calaveras and San Andreas fault zones.

In the area of the August 6, 1979 earthquake the Calaveras fault zone borders the west side of the Diablo Range. The fault runs within low foothills on the east side of Santa Clara Valley. The fault zone forms a northwest-trending trench in which Coyote Lake and Anderson Lake are impounded. Eastward-dipping Great Valley sequence sandstones, shales, and conglomerates of Cretaceous age east of the Calaveras fault zone are juxtaposed against small bodies (locally fault-bounded) of serpentine, Jurassic-Cretaceous Franciscan Assemblage shale, Tertiary volcanics, and Pliocene and Pleistocene sandstones, shales, and conglomerates (Fig. 2). North of Hollister the Calaveras crosses the southern end of the Santa Clara Valley, offsetting both late Pleistocene and Holocene alluvium. The fault zone is vertical to nearly vertical in practically all exposures.

Right-lateral movement along the fault is demonstrated by the offset of correlative rocks, streams, and even streets, sidewalks, and curbs. A minimum of 0.14-0.71 cm/yr of slip has been determined from offset 3.5-m.y.-old volcanic rocks east of Gilroy (Nakata, 1977), but the long-term slip rate is believed to be between 1.2 and 1.7 cm/yr (Herd, 1978). Creep rate along the Calaveras fault has been documented by Savage and Burford (1973) and Wesson et al. (1974). At Hollister, about 0.5 cm/yr of tectonic creep (fault creep) has been documentated along the Calaveras fault zone. East of Gilroy, in the area of the August 6, 1979 earthquake, between 1.0 and 1.2 cm/yr of fault creep has been detected on the Calaveras. Northeast of San Jose the creep rate on the Calaveras decreases to only 0.25 cm/yr.

The Calaveras fault zone has been active throughout the late Quaternary. At least one historic earthquake (July 3, 1861) was accompanied by surface rupture along an unknown length of the fault east of Oakland (Brewer, 1930;

Trask, 1864; Whitney, 1865). Aligned landforms, characteristically associated with active strike-slip faults (scarps, sag ponds, linear valleys, trenches, offset streams) delineate a narrow zone (generally less than 0.1 km wide) of both left- and right-stepping, en enchelon, recently active breaks in the Calaveras fault zone (see Fig. 6). Through Hollister, the recently active trace of the Calaveras fault zone strikes N.21°W. At the edge of the Diablo Range at San Felipe Lake the Calaveras fault zone abruptly turns west trending N.27°W. As it turns, a number of secondary recently active breaks splay westward from the main fault. At Coyote Lake, just west of the epicenter of the principal August 6, 1979 shock, the recently active trace of the Calaveras fault zone steps abruptly eastward (right-stepping) about 0.3 km (see Fig. 6).

SURFACE FAULTING

Discontinuous surface faulting was observed along a 14.4-km length of the Calaveras fault zone east of Gilroy, California, following the Coyote Lake earthquake (Herd and others, 1979). Fresh en echelon fractures in pavement and soil were discovered at several localities along the recently active trace of the fault, locally superimposed on older cracks and breaks. The discontinuous rupture extended northwestward from a point about 5 km southeast of San Felipe Lake (nearly opposite the southernmost aftershock epicenter shown in Fig. 6) to within 6 km of the main shock. No surface faulting was seen in the epicentral area near Coyote Lake. A maximum offset of 5 mm was measured in right-laterally offset curbs along California Highway 152 at the north edge of San Felipe Lake. A creepmeter at the south end of the surface break (see Fig. 1) measured 4.2 mm coseismic slip event, but it is unclear if the record was contaminated by hysteresis during the strong shaking of the instrument. That creepmeter recorded an additional 4 mm of displacement within 24 hours of the main shock.

SEISMOGRAPH STATIONS AND DATA PROCESSING

The Coyote Lake earthquake and its aftershocks occurred near the center of the USGS Central California Microearthquake Network (Figure 3). There are over 50 high-gain and 6 low-gain three-component short-period seismic stations within a radius of 50 km of this earthquake. Complete analysis of the entire data set will take time; here we have concentrated our initial efforts in studying a selected subset of the existing data. Twenty-one close in stations were chosen to provide adequate azimuthal coverage of the studied earthquakes. They are shown in Figure 4 together with stations in the USGS Microearthquake Network that are not used in the earthquake location. However, we have read data from additional stations in the USGS Network for selected events in order to provide better coverage in determining focal mechanisms.

Over 1,000 locatable aftershocks were recorded in the first 15 days of the main shock. A list of the larger aftershocks has been prepared from the daily monitor records by Jerry Eaton (personal communication, 1979). We selected events of signal duration 30 sec or larger in Eaton's list to be processed and analyzed. This provides a coverage of aftershocks of magnitude 2 and greater, except for a few cases where the earthquake occurred in the coda of a previous event. In addition, some smaller aftershocks were included especially in the first hour of the main shock and to fill in quieter periods.

First P-arrival, first P-motion, and signal duration (to a point where the signal amplitude no longer exceeds twice the amplitude of the background) were read on seismograms recorded on 16 mm films using a Geotech viewer

(20x magnification). Timing precision was about ±0.05 sec, and stations with poor quality arrivals were usually ignored. Additional data were provided by Jerry Eaton on the mainshock (where he timed all the stations from playback records of the analog magnetic tapes), and by Bill Ellsworth, Sharon Kirkman, and Janice Murphy for some of the aftershocks.

A total of 150 earthquakes were studied, 6 of which were located well outside the aftershock area. There was no prominent foreshock activity, although an earthquake of magntidue 2.2 did occur 2.5 hours before the main shock on the Sargent fault about 10 km southwest of the aftershock zone. In November, 1974 a magnitude 5.1 earthquake occurred on the Busch fault, which lies between the Sargent and Calaveras fault and conjugate to them about 25 km south of the August 6 mainshock (see Fig. 1).

CRUSTAL MODELS AND EARTHQUAKE LOCATIONS

The HYPO71 computer program (Lee and Lahr, 1972/1975) and its modified version HYPO74 were used to locate hypocenters, compute magnitudes, and plot first-motion diagrams. These programs compute traveltimes assuming a horizontally layered crustal model, and thus provide only approximate hypocenter locations in a laterally inhomogeneous region such as that in which the Coyote Lake earthquake occurred (see Fig. 2).

The routine locations of earthquakes by the USGS Central California Microearthquake Network in this area place the epicenters about 3 km east of the Calaveras fault trace. From geological evidence, the Calaveras fault is nearly vertical. If earthquakes did occur on the fault, then such displaced

locations can be explained by the fact that Franciscan rocks of high seismic velocity are exposed east of the Calaveras fault whereas they are overlain by younger sedimentary rocks of low seismic velocity west of the fault. By seismic ray-tracing techniques, Engdahl and Lee (1976) demonstrated that velocity contrast across a fault can cause a few kilometers bias in earthquake location in the direction of high velocity material. Large velocity contrast in the area of the Calaveras fault has been discussed by Mayer-Rosa (1973).

To simulate the seismic velocity contrast across the Calaveras fault, we constructed 6 simplified horizontally layered models based on existing explosion data and surface geology, and assigned the selected 21 seismic stations to one of these models based primarily on geographical location as shown in Figure 5. In the first analysis, we assumed no station corrections in locating earthquakes. P residuals from the located events indicate minor station corrections (see Table 1) and they were applied in the second analysis. Location differences between the first and second analyses are about 0.5 km. Results of the second analysis are shown in Table 2. The root-mean-square traveltime residual of most earthquakes is about 0.1 sec. Precision is about 0.5 km in epicenter location and about 1 km in focal depth. These precision estimates are with respect to the assumed crustal model. Experience with locations of known explosions in this region suggests that relative epicenter error is probably better than 1 km.

HYPOCENTER DISTRIBUTION

The earthquake epicenters listed in Table 2 are plotted on a 1:24,000 scale map for working purposes. Figure 6 shows the distribution of these earthquakes on a reduced scale map. The distribution of the epicenters suggests that the Coyote Lake earthquake sequence occurred on the Calaveras fault. The main shock occurred near the northern end of Coyote Lake. Aftershocks occurred mostly south of the main shock for a distance of about 20 km along the Calaveras fault. Of the 143 aftershocks located, only 9 occurred northwest of the main shock and they extended a distance of about 5 km along the fault.

To illustrate the hypocenter distribution a straight line approximating the surface trace of the Calaveras fault was constructed between points A & A' as shown in Figure 6. Earthquake hypocenters were projected onto this cross section. The result, shown in Figure 7, suggests that aftershocks occurred primarily along a 25 km section of the Calaveras fault from 4 km to 12 km deep. A tranverse view of this cross section, shown in Figure 8, suggests that aftershocks occurred in a vertical section about 4 km wide centered on the fault trace. However, this width may not reflect the actual width of the fault zone because some scatter of the earthquake foci could be caused by location errors.

The aftershocks (Fig. 6) appear to cluster in two linear trends that are offset about 2 km near lat 37 02.5'. The earthquake pattern suggests that the Calaveras fault zone near Gilroy consists of two right-stepping fault breaks. Surficially, however, the recently active trace of the Calaveras

through that latitude strikes uniformly N.27°W. The fault zone deflects in trend only near lat 37°06', where the fault steps eastward about 0.3 km. Neither the amount of the surficial right step or its location are compatible with the present aftershock locations presented here. Either the recently active surficial trace of the Calaveras fault zone near Gilroy does not precisely reflect the fault geometry at depth, or the aftershock offset is due to earthquake mislocation.

MAIN SHOCK AND MAGNITUDE OF AFTERSHOCKS

Parameters of the main shock are:

Origin time: August 6, 1979, $17^h05^m22.3^s$ ($\pm$ 0.1 sec)

Epicenter: 37° 6.7'N, 121°32.0'W ($\pm$ 1 km)

Focal depth: 9.6 km ($\pm$2 km)

Magnitude: 5.7 ($\pm$ 0.2) based on 11 readings of signal durations (Lee, Bennett, and Meagher, 1972). The seismographic stations of the University of California gives a Richter magnitude of 5.9 using a 100x Wood-Anderson record at Berkeley (Uhrhammer, 1979).

The coordinates of the mainshock epicenter, as determined by Uhrhammer (1979), place it approximately 3 km southeast of our location and our focal depth is 3 km deeper. Seismic moment of the mainshock was determined as 4.7×10^{24} dyne-cm by Langston (written communication, 1979) and as 6×10^{24} dyne-cm by Uhrhammer (1979).

In Table 2, magnitudes of earthquakes studied were estimated from signal durations using a similar procedure described by Lee, Bennett and Meagher (1972). A comparison with the magnitudes of 29 earthquakes given by Uhrhammer (1979) indicated that our magnitudes were 0.2 units higher. To study the aftershock magnitudes and their variations with time, signal durations were read using the daily monitor record of the station at Chesbro Reservoir (JCB), which is located about 15-20 km west of the after-

shock zone (see Fig. 4). The daily monitor is a helicorder record 90 cm long, and signal durations are read to a point where the signal amplitude no longer exceeds 3 mm. The 3 mm amplitude of the trace has been chosen because of the microsesimic noise at JCB. The duration magnitudes obtained from this station usually agree to $\pm$0.1 magnitude units of those determined using several stations. A list of aftershocks with magnitudes equal or greater than 1.0 was prepared from the duration data. The cumulative number of events (N) with magnitude M and larger is plotted against magnitude (M) in Fig. 9. The graph suggests the JCB catalog is complete to the M = 1 threshold. The straight line fit to the data obtained by inspection for M between 1 and 3.5 is:

$$\log N = 3.33 - 0.74 M$$

In order to quantify the aftershock activity, the difference between the magnitudes of the mainshock (M) and the largest aftershock (M_1) has been considered. For the Coyote Lake sequence, the magnitude of the largest aftershock in the first 15 days is 4, so that $M - M_1$ is about 1.7 to 1.9. For seismic sequences of earthquakes occurring in Greece and surrounding regions, with $M \geq 5.7$ and focal depths varying from 15 to 42 km, Papazachos et al (1967) obtained the formula:

$$M_1 = 1.07 + 0.71 M$$

By using this formula, a value of M_1 = 5.1 to 5.2 is obtained. Bath observed differences between M and M_1 of the order of 1.2 units of magnitude (Richter 1958).

Assuming the energy-magnitude relationship, $\log E = 11.8 + 1.5 M$ (Richter, 1958) and the magnitude of 5.9 for the mainshock and the magnitudes of Table 2 for the aftershocks, the energy released by the mainshock is 4.5×10^{20} ergs and the total seismic energy released by the aftershocks through August 21 is 3.0×10^{18} ergs. The ratio of the

aftershock energy to that of the mainshock is 0.007, close to the lower limit of the normal observed range of 0.001 to 0.5 (Benoiff, 1951, Utsu, 1961). Thus we conclude that the number and size of aftershocks for the Coyote Lake sequence are much less than that expected for a main shock of magnitude 5.7 to 5.9. This may be explained in several ways: 1) this earthquake sequence may be different than a typical sequence because it occurred in creeping fault zone where not all the strain energy release is in the form of sudden earthquake events, or 2) aftershocks for the Coyote Lake earthquake are not yet over and our first 15 days are not adequate to describe this earthquake sequence.

Figure 10 shows the number of aftershocks per day (n) plotted against time (t) on a double logarithmic diagram as suggested by Utsu (1961). The modified Omori formula is:

$$n(t) = K/(t + c)^p$$

where K, c, and p are constants. Normal observed values for p and c are from 0.9 to 1.3 and 0.01 to 2 days, respectively (Utsu, 1961). Referring to the constant c, Page (1968) attributes the observed values to the incompleteness in the data at the beginning of the sequence rather than some real feature in the aftershock process and such bias leads to a value of c greater than zero. Studies of many sequences did not suggest any relationship between p and M, p and $M - M_1$ (Utsu, 1961). Lower values of p have been observed for deeper earthquakes (Gibowicz, 1973). In the present case p is about 0.82 from Figure 10. The decay in aftershock activity with time reflects a decrease of stress in the aftershock region. Perhaps the low value of p for this sequence, indicating a longer decay time, is related to the creeping nature of the fault zone.

The temporal variation of b-value of the Coyote Lake earthquake sequence was investigated by computing b-value using sets of 50 events according to:

$$b = 0.434/(\overline{M} - M_{min})$$

Where $\overline{M}$ is the average magnitude and M_{min}, the minimum magnitude. This formula derived by Utsu (1965) is an approximation of the maximum likelihood method, and is valid when the difference between the maximum and minimum magnitudes of an earthquake data set is greater than 2 units of magnitude. The 95% confidence limits for the estimate of b are $\pm$ 1.96 b/$\sqrt{n}$, where n is the number of events considered in the data set (Aki, 1965).

Gibowicz (1973) and Cagnetti and Pasquale (1979), studying other seismic sequences, found that the b-value increases after a large earthquake and decreases before another in the same sequence. Experiments in rock deformation suggest a similar result: the value of b(t) decreases as stress increases (Scholz, 1968). In the study of the Danville earthquake swarm of 1970, Bufe (1970) found an inverse correlation between the value of b and strain release.

In Figure 11, 3 sets of data are plotted versus time: (a) the daily maximum magnitude, (b) the b-value, and (c) the daily number of events (magnitude $\geq$ 1). The time axis is in days after the mainshock. Comparison between Figure 11(a) and 11(b) suggests that larger aftershocks seem to occur when the b-value is at a minimum. This phenomenon has been reported by Gibowicz (1973) and Cagnetti and Pasquale (1979) for two other earthquake sequences.

SOURCE PARAMETERS OF SOME AFTERSHOCKS

Some aftershocks that span the duration magnitude range $0.8 \leq M_D \leq 3.4$ were selected for spectral analysis. The dynamic range for recording these events was achieved by using low-gain stations in the USGS Central California Microearthquake Network (see Fig. 4) as well as stations at different distances. P-wave spectra were obtained from vertical-component seismographs while S-wave spectra were obtained from horizontal component seismographs (see Figure 12). Window lengths were selected by inspection and ranged from 1 to 5 sec in duration. A cosine taper of 0 and 5 percent was applied to the onset of the P and S waves respectively: the P- and S-wave windows were terminated with a 5 percent cosine taper. The Fourier transform of the windowed signal was then corrected for instrument response (Bakun and Dratler, 1976).

The source-displacement spectrum is obtained from the P and S displacement spectra by the relations given in Bakun and Lindh (1977, p. 621) using α = 6.0 km/sec, β = 3.5 km/sec, ρ = 2.8 gm/cc, and $Q_\alpha = Q_\beta$ = 200. The seismic moment M_o is given by the long-period level of the source-displacement spectrum as illustrated in Figure 13. Corner frequencies were estimated by inspection from the S-wave source-displacement spectra (Figure 13) for those shocks for which consistent well-defined spectral corners were available for at least two recording sites located in differing azimuthal quadrants. Source radii and stress-drop estimates were obtained following Brune (1970; 1971). Results from this initial analysis yield stress drops between 0.9 and 4.2 bars

for earthquakes with seismic moments between 7×10^{19} and 9×10^{20} dyne-cm (see Table 3). An examiniation of seismic moment Mo versus coda duration magnitude suggests that the moment-magnitude relationship obtained by Bakun and Lindh (1977) for the Oroville, California region ($\log Mo = 1.21M + 17.02$) is appropriate for the Coyote Lake section of the Calaveras fault.

FOCAL MECHANISM OF MAIN SHOCK AND SOME AFTERSHOCKS

Individual nodal-plane solutions were obtained for the main shock (Fig. 14) and more than 50 aftershocks by manual fits to first P-motion data plotted on the lower focal hemisphere in an equal-area projection. Only the better focal mechanism solutions for the aftershocks are shown (in Fig. 15). First P-motion readings of the main shock were read by Jerry Eaton from playback records of analog magnetic tapes. However, because the HYPO74 program limits the maximum number of phase cards to 100, only a subset of Eaton's data were used in the nodal-plane solution. Since we have assigned a crustal structure model to only 21 selected stations for location purposes, other stations were arbitrarily given a nominal crustal model. A few first P-motions are inconsistent with the nodal-plane solutions. These may be due to either station polarity reversal or inadequate modeling of the crustal structure.

Figure 14 shows the nodal-plane solutions for the main shock. The preferred fault-plane strikes N 20° W and dips 90°; the motion is right-lateral strike-slip. The trend of the surface trace of the

Calaveras fault in the vicinity of the Coyote Lake is approximately N 25° W. Therefore the focal mechanism of the main shock agrees well with the local geology that the Calaveras fault is a near vertical, right-lateral strike-slip fault. Focal mechanisms of most aftershocks studied so far agree with that of the main shock. These results are illustrated in Figure 15.

DISCUSSION

The August 6, 1979 Coyote Lake earthquake and its major aftershocks occurred along the Calaveras fault zone. The focal mechanism of the main shock is consistent with a nearly vertical, right-lateral strike-slip fault like the Calaveras. The aftershocks are aligned in a nearly vertical northwest-trending band that either locally coincides with or broadly parallels the strike of the Calaveras fault zone. There are no other faults nearby which have a history or sense of movement consistent with the Coyote Lake earthquake and its aftershocks. The nearest northwest-trending fault, the Madrone Springs fault (see Fig. 2), lies more than 5 km east of the main shock. That fault is a high-angle reverse fault (east side up), separating Franciscan Assemblage rocks on the east from Great Valley sequence sandstones, shales, and conglomerates. The Madrone Springs fault displays no evidence of late Quaternary activity. The location of the main August 6, 1979 shock about

1 km east of the Calaveras fault zone may be accounted for by the difficulties in accurately modeling seismic wave propagation in this geologically complex region. That is, the displacement of the epicenter to the east of the fault trace may be the bias introduced by incorrectly modeling the local crustal structure in the location program.

The number and size of aftershocks accompanying the Coyote Lake earthquake are much less than that expected for a main shock of magnitude 5.7 $\pm$ 0.2 based on argument in energy presented above. A portion of the strain energy might have been released by fault creep, or there might be more aftershocks for the Coyote Lake earthquake. One cannot rule out the possibility that the August 6 earthquake is a forerunner of a larger earthquake yet to follow.

It is interesting to note that the Coyote Lake earthquake appears to be the fourth in a series of moderate-sized ($M \geq 5$) earthquakes that have migrated northward along the central California segment of the San Andreas fault system. The Parkfield-Cholame earthquake of magnitude 5.5 occurred along the San Andreas fault zone on June 28, 1966. That earthquake was followed by one (magnitude 5.0) about 120 km north at Bear Valley on February 24, 1972. On Thanksgiving Day, November 28, 1974, a magnitude 5.1 shock was centered on the Busch fault, a small fault which lies between the San Andreas north of Bear Valley and the Calaveras fault zone, conjugate to them. The aftershocks of the 1979 Coyote Lake earthquake extend south to the intersection of the Busch and Calaveras faults. The apparent northward migration of moderate-sized earthquakes on the San Andreas-Calaveras fault system was first noted by Wood and

Allen (1973), who predicted a $M \geq 5.0$ earthquake would occur within the San Andreas system near latitude 37° before 1978. These moderate sized earthquakes appear to be moving northward from the San Andreas fault zone to the Calaveras, along the east side of the Humboldt plate (Herd, 1978). Waves of slip migrating northward from the San Andreas fault to the Calaveras fault is consistent with the model of creeping faults proposed by Bakun et al (1980). If this earthquake migration pattern continues, the next moderate sized earthquake in central California should occur north of Coyote Lake along either the northern Calaveras fault zone, or the Hayward fault zone, which branches to the west.

ACKNOWLEDGEMENTS

We thank Jerry Eaton for providing us with a list of aftershocks from the daily monitor records and his readings of the main shock. We are grateful to Bill Ellsworth, Sharon Kirkman, and Janice Murphy for reading some of the seismograms , and to Mari Gunn, Carol McHugh, Catherine McMaster, Bob Nowack, and Judy York for general assistance. We wish to thank Earl Brabb, Rob Cockerham, Jerry Eaton, Dave Hill, Bob Page, Russ Robinson and Wayne Thatcher for their comments on the manuscript.

We are grateful to C.A. Langston and R.A. Uhrhammer who kindly made available their results prior to publication.

REFERENCES

Aki, K., 1965, Maximum likelihood estimate of b in the formula log N = A - bM and its confidence limits: Bull. Earthquake Research Inst., Tokyo Univ., v. 43, p. 237-239.

Bakun, W. H. and J. Dratler, 1976, Empirical transfer functions for stations in the central California seismological network: USGS Open-file Report, 76-259.

Bakun, W. H. and A. H. Lindh, 1977, Local magnitudes, seismic moments, and coda durations for earthquakes near Oroville, California: Bull. Seism. Soc. America, v. 67, p. 615-629.

Bakun, W. H., R. M. Stewart, C. G. Bufe, and S. M. Marks, 1980, Implication of seismicity for failure of a section of the San Andreas fault: Bull. Seism. Soc. America, in press.

Benoiff, H., 1951, Earthquakes and rock creep. Part I: Creep characteristics of rocks and the origin of aftershocks: Bull. Seism. Soc. America, v. 67, p. 31-62.

Brewer, W. H., 1930, Up and down California in 1860-64; the journal of William H. Brewer (F. P. Farquahar, ed.): New Haven, Yale Univ. Press, 601 p.

Bufe, C., 1970, Frequency-magnitude variations during the 1970 Danville earthquake swarm: Earthquake Notes, v. 51, p. 3-7.

Cagnetti, V. and V. Pasquale, 1979, The earthquake sequence in Friuli Italy, 1976: Bull. Seism. Soc. America (in press).

Engdahl, E. R. and W. H. K. Lee, 1976, Relocation of local earthquakes by seismic ray tracing: J. Geophys. Research, v. 81, p. 4400-4406.

Gibowicz, S. J., 1973, Variations of the frequency-magnitude relation during earthquakes in New Zealand: Bull. Seism. Soc. America, v. 63, p. 517-528.

Herd, D. G., 1978, Neotectonic framework of central coastal California and its implications to microzonation of the San Francisco Bay region, in Proceedings of the Second International Conference on Microzonation for Safer Construction--Research and Application, San Francisco, California, November 26-December 1, 1978, v. 1, p. 231-240.

Herd, D. G., McLaughlin, R. J., Sarna-Wojicki, A. M., Lee, W. H. K., Sharp, R. V., Sorg, D. H., Stuart, W. D., and Harsh, P. W., 1979, Surface faulting accompanying the August 6, 1979 Coyote Lake earthquake: Secondary fault movement? (abst.): EOS, in press.

Jennings, C. W., 1977, Geologic map of California: California Division of Mines and Geology, California Geologic Data Map Series, 1 sheet, scale 1:750,000

Lee, W. H. K., and J. C. Lahr, 1972/1975, HYP071 (revised): A computer program for determining hypocenter, magnitude, and first motion pattern of local earthquakes: USGS Open-file Report, 75-311.

Lee, W. H. K., R. E. Bennett, and K. L. Meagher, 1972, A method of estimating magnitude of local earthquakes from signal duration: USGS Open-file Report.

Mayer-Rosa, D., 1973, Travel-time anomalies and distribution of earthquakes along the Calaveras fault zone, California: Bull. Seism. Soc. America, v. 63, p. 713-729.

Nakata, J. K., 1977, Distribution and petrology of the Anderson-Coyote Reservoir volcanic rocks: San Jose State Univ., California, Master of Science Thesis, 105 p.

Page, R., 1968, Aftershocks and microaftershocks of the great Alaska earthquakes of 1964: Bull. Seism. Soc. America, v. 58, p. 1131-1168.

Papazpchos, B., N. Delibovsis, N. Liovpis, G. Moumoulidis and G. Purcaru, 1967, Aftershock sequences of some large earthquakes in the region of Greece: Ann. Geofis. Rome, v. 20, p. 1-93.

Radbruch-Hall, D. H., 1974, Map showing recently active breaks along the Hayward fault zone and the southern part of the Calaveras fault zone, California: USGS Miscellaneous Investigations Series Map I-813, 2 sheets, scale 1:24,000.

Richter, C. F., 1958, Elementary seismology: Freeman, San Francisco.

Rogers, T. H., and R. D. Nason, 1971, Active displacement on the Calaveras fault zone at Hollister, California: Bull.Seism. Soc. America, v. 61, p. 399-416.

Savage, J. C. and R. O. Burford, 1973, Geodetic determination of relative plate motion in central California: J. Geophys. Research, v. 78, no. 5, p. 832-845.

Scholz, C., 1968, The frequency-magntiude relation of microfracturing in rock and its relation to earthquakes: Bull. Seism. Soc. America, v. 58, p. 399-415.

Trask, J. B., 1864, Earthquakes in California from 1800 to 1864: California Academy of Sciences Proceedings, v. 3, p. 130-153.

Uhrhammer, R. A.. 1979, Observations of the Coyote Lake, California earthquake sequence of August 6, 1979: Draft copy.

Utsu, T., 1961, A statistical study on the occurrence of aftershocks: Geophys. Mag., v. 30, p. 521-605.

Utsu, T., 1965, A method for determining the value of b in a formula log n = a - bM showing the magnitude-frequency relation for earthquakes: Geophys. Bull., Hokkaido Univ., v. 13, p. 99-103.

Wesson, R. L., E. J. Helley, K. R. Lajoie, and E. M. Wentworth, 1975, Faults and future earthquakes, in Borcherdt, R. D., ed., Studies for seismic zonation of the San Francisco Bay region: USGS Professional Paper 941-A, p. A5-A30.

Whitney, J. D., 1865, Geology of California, v. I, part I. Geology of the Coast Ranges: California Geological Survey, p. 1-197.

Wood, M. D., and S. S. Allen, 1973, Recurrence of seismic migrations along the central California segment of the San Andreas fault system: Nature v. 244, no. 5413, p. 213-215.

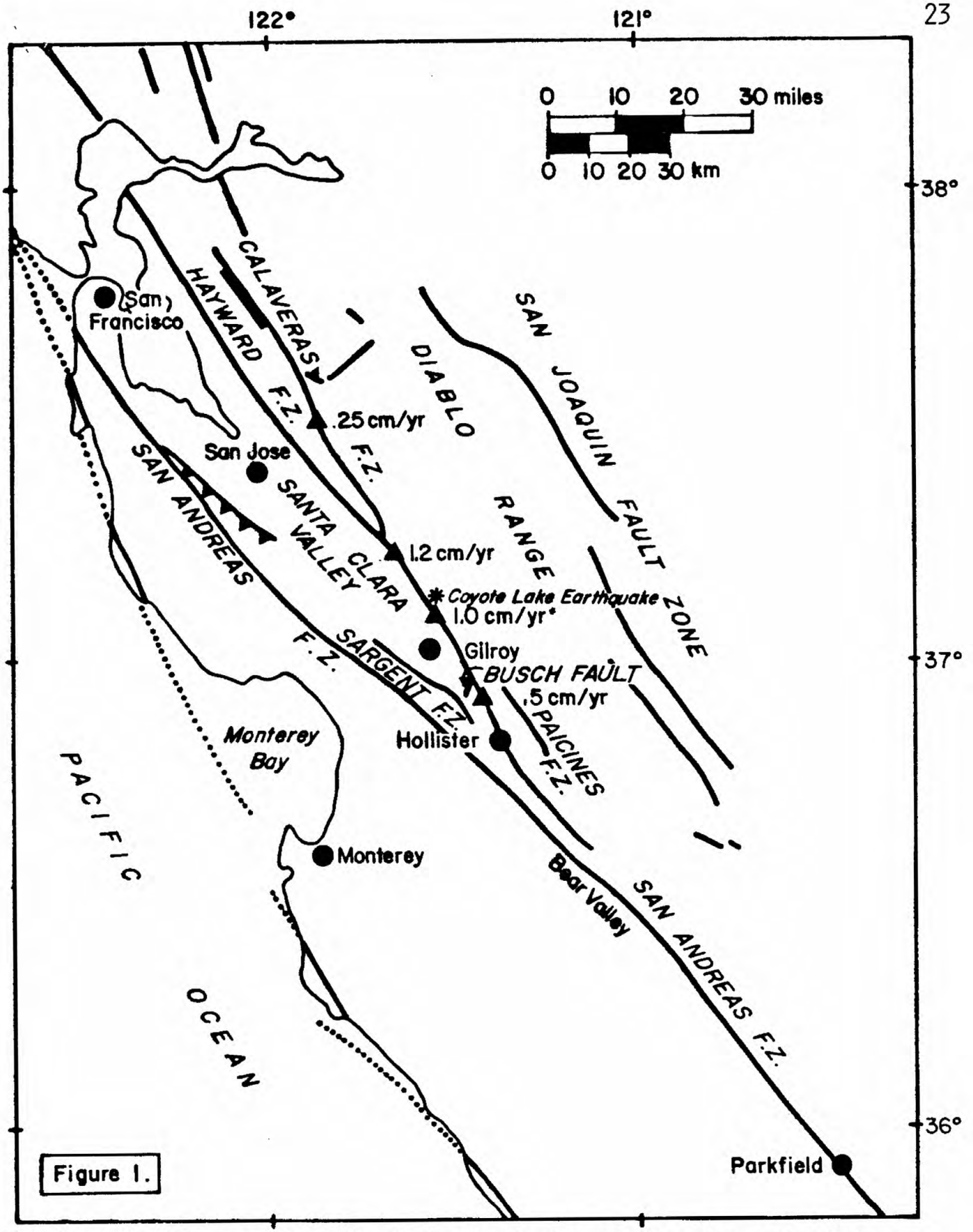

FIGURE 1.--Principal recently active faults in the San Francisco Bay region (after Herd, 1978), showing the location of the Aug. 6, 1979 earthquake (✳). Triangles denote fault creep rates from Wesson et al (1974) (unmarked) and Savage & Burford (1973) (*). The approximate position of the July 1861 rupture on the Calaveras fault zone is shaded.

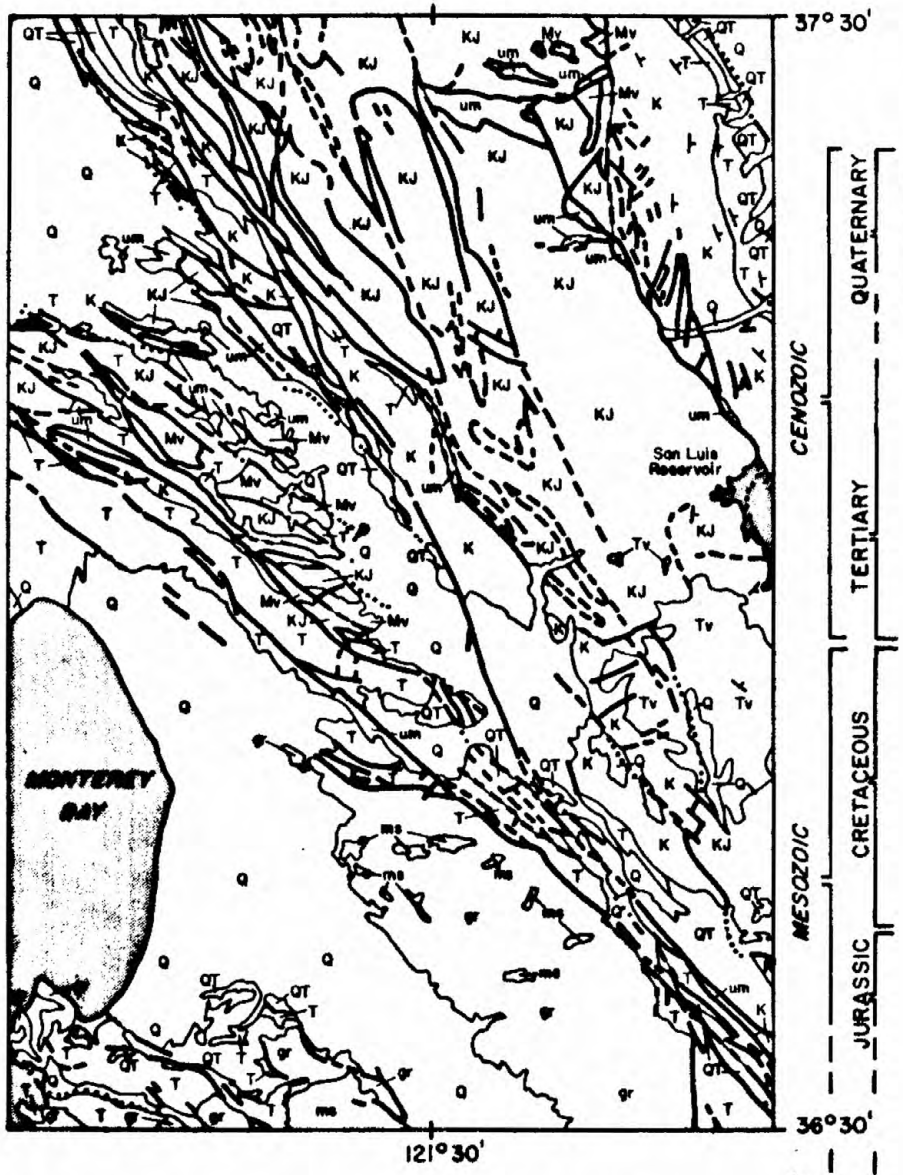

Figure 2. --Generalized geologic map of the Gilroy, California area (after Jennings, 1977).

GEOLOGIC LEGEND
(GENERALIZED DESCRIPTION OF ROCK TYPES)

CENOZOIC — QUATERNARY — Pleistocene - Holocene

Q — Alluvium; unconsolidated and semi-consolidated.

QT — Sandstone, shale, and gravel; loosely consolidated.

CENOZOIC — TERTIARY

T — Sandstone, shale, siltstone, and conglomerate; moderately to well consolidated.

Tv — Volcanic flow rocks.

MESOZOIC — CRETACEOUS

K — Great Valley Sequence: sandstone, shale, and conglomerate.

Mv — Volcanic flow rocks, greenstone.

gr — Granite.

MESOZOIC — JURASSIC

KJ — Franciscan Assemblage: sandstone with minor shale, chert, limestone, and conglomerate; melange of fragmented Franciscan Assemblage rocks.

um — Ultramafic rocks, mostly serpentine.

PALEOZOIC — PERMIAN

ms — Metasediments: slate, quartzite, chert, and marble.

SCALE 1:750,000

0 10 20 30 40 miles

0 10 20 30 40 km

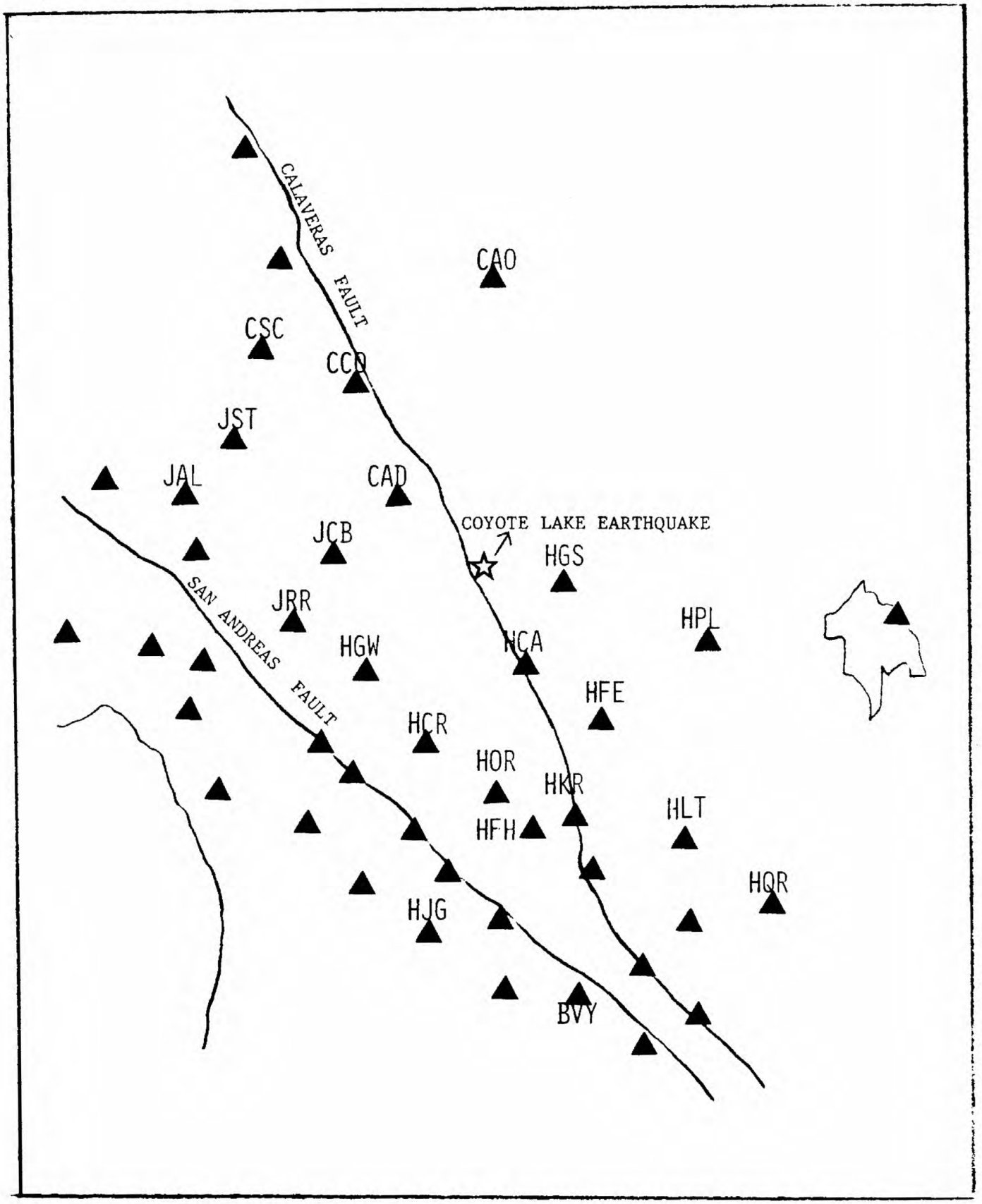

FIGURE 4. Map showing seismic stations used in earthquake location (stations with three letter code), and other USGS seismic stations in the area. Three-component low-gain stations are at CAO, HPL, HQR, and JAL.

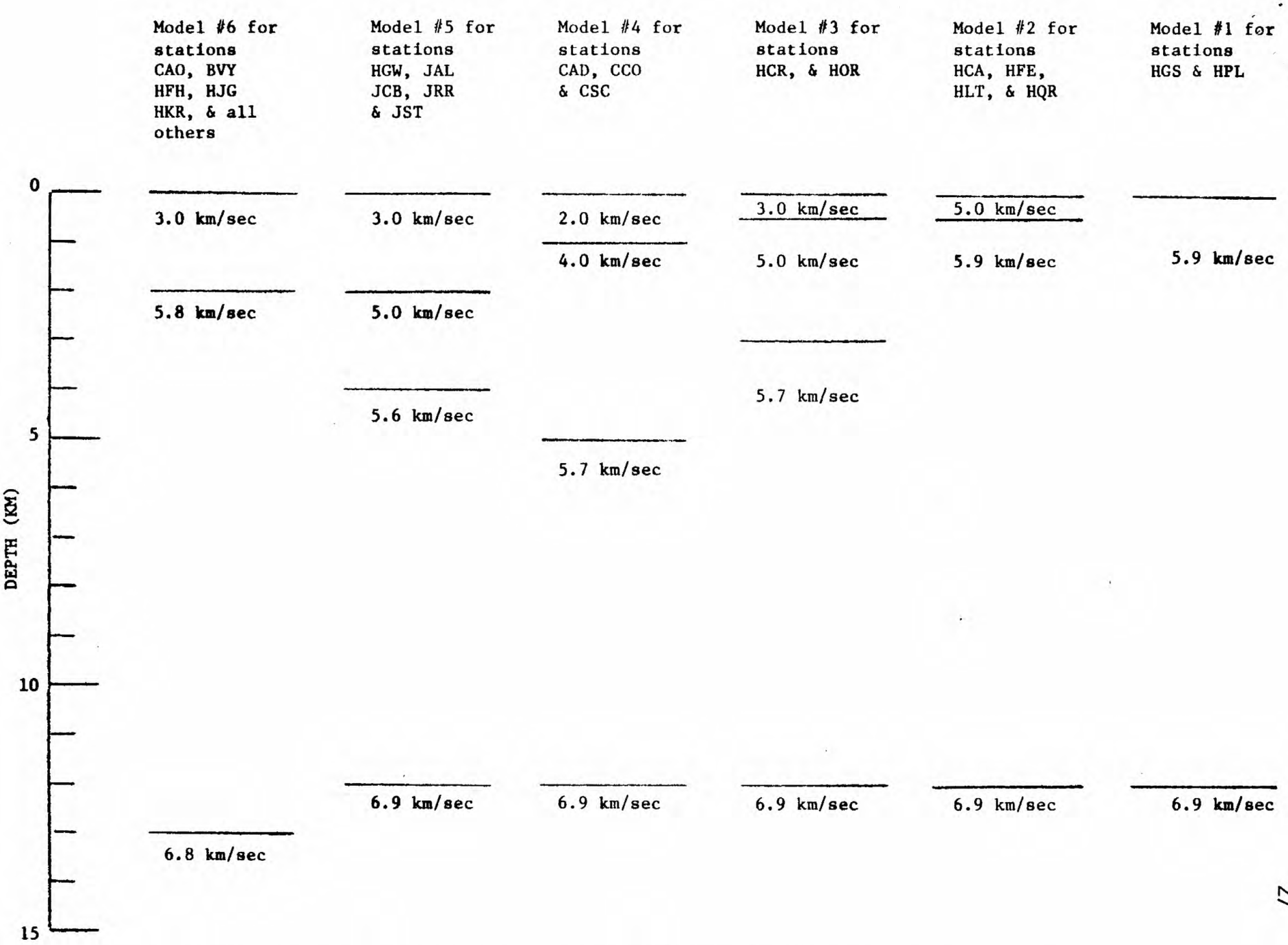

FIGURE 5. Crustal structure models for stations used in earthquake location.

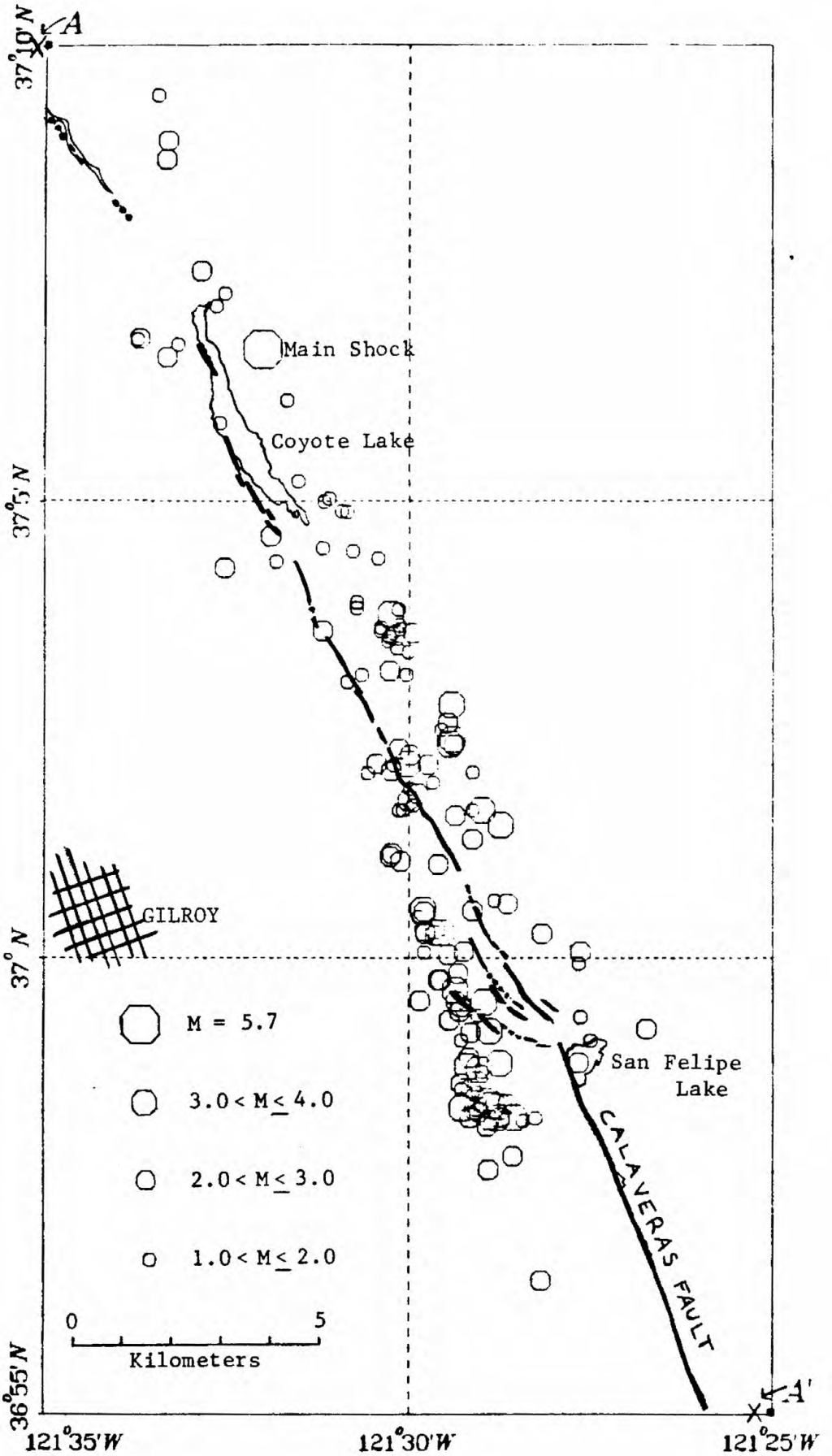

FIGURE 6. Map showing epicenters of Coyote Lake earthquakes (August 6 to 21, 1979).

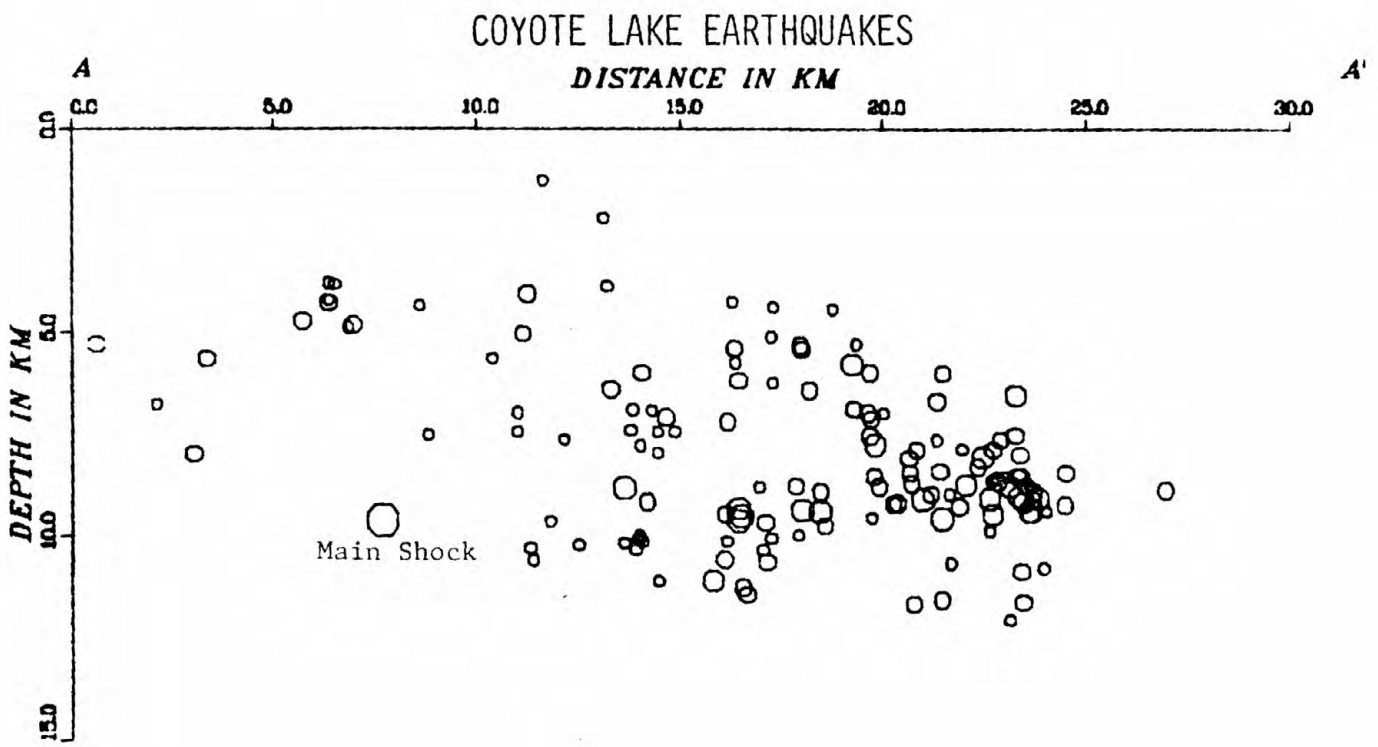

FIGURE 7. Cross-sectional plot of hypocenters along line A-A' (see FIG. 6).

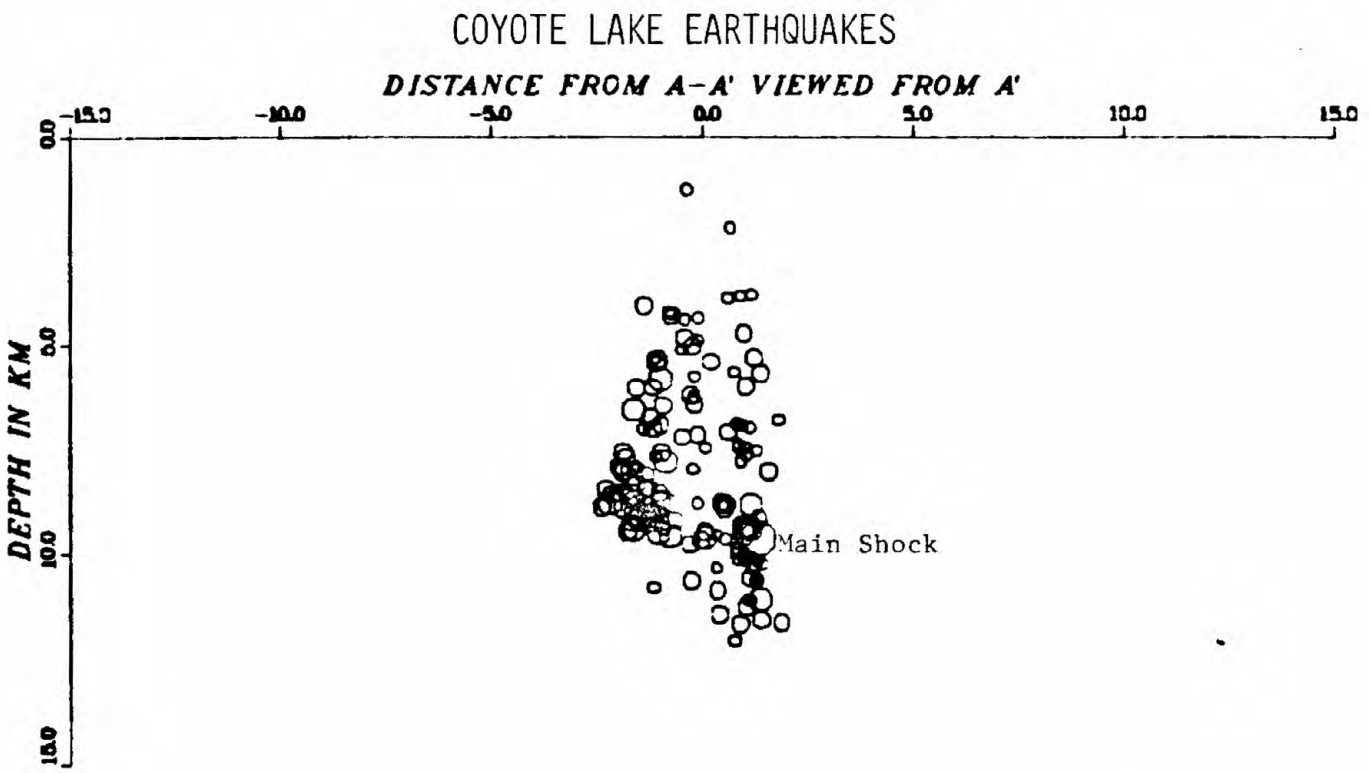

FIGURE 8. Transverse view of the cross-sectional plot along A-A' as viewed from A' (see FIG. 6 for position of A & A').

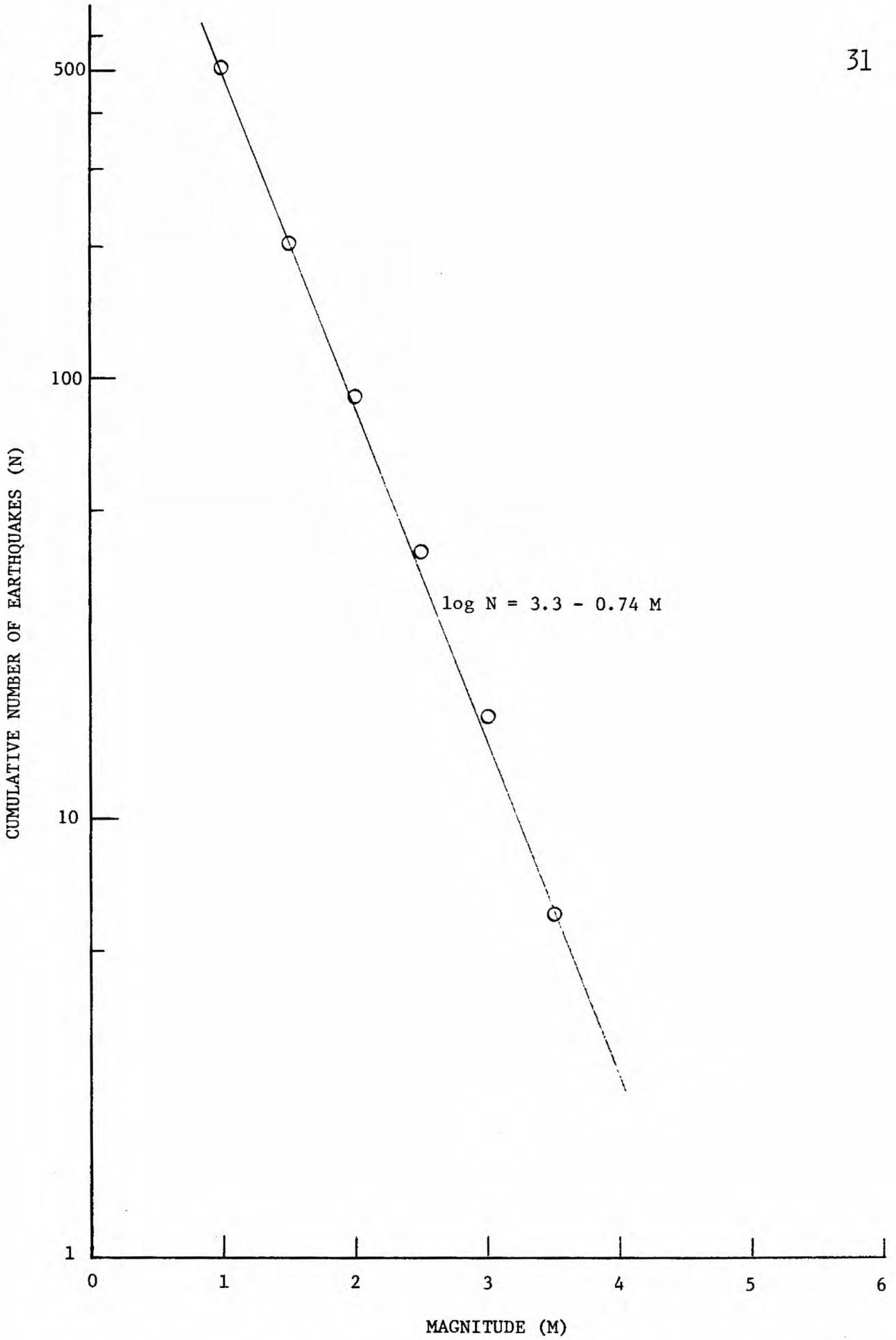

FIGURE 9. Cumulative number of earthquakes vs magnitude for Coyote Lake aftershocks.

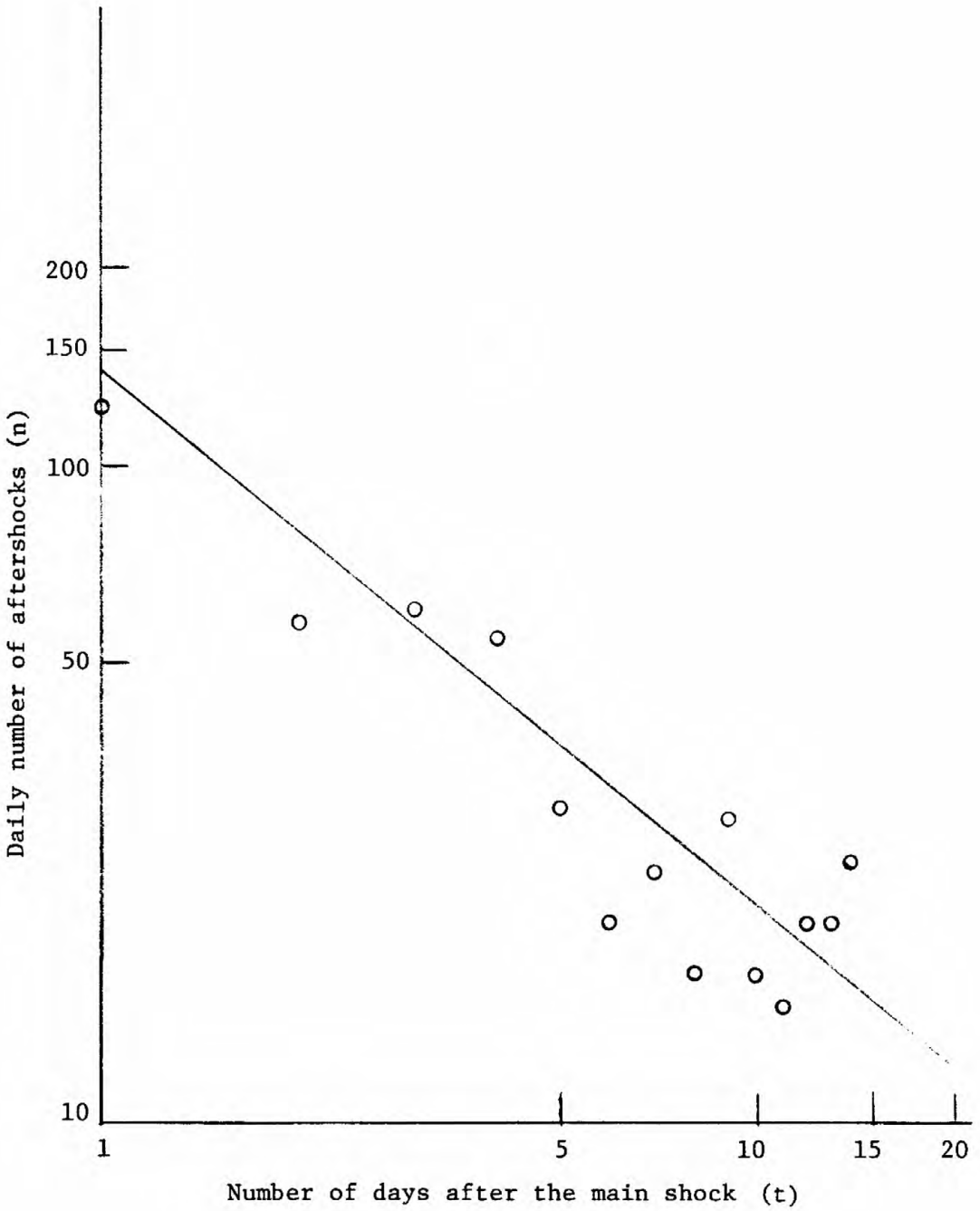

FIGURE 10. Daily number of aftershocks as a function of time after the main shock.

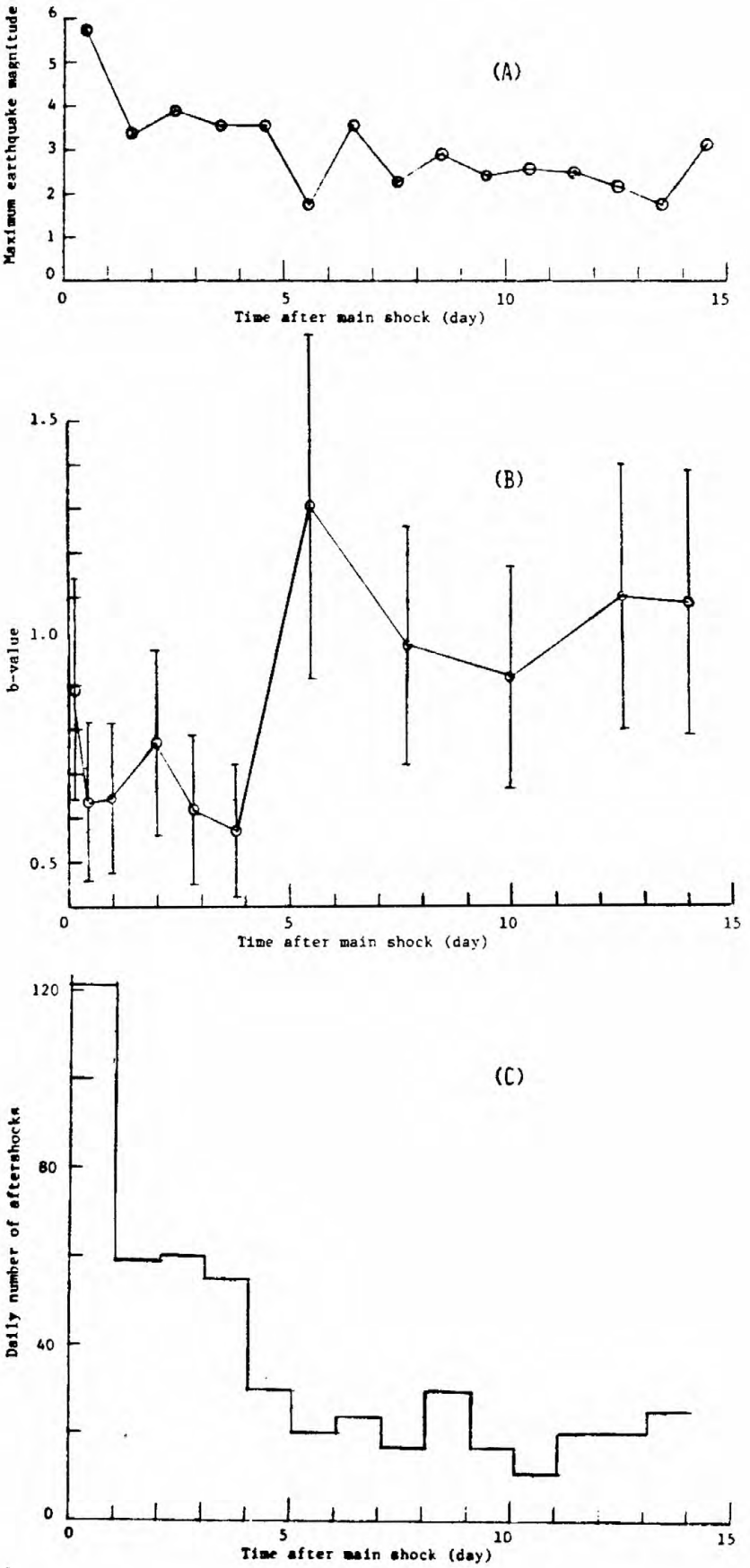

FIGURE 11. (A) Maximum earthquake magnitude vs time after main shock.
(B) b-value as a function of time after main shock.
(C) Daily number of aftershocks.

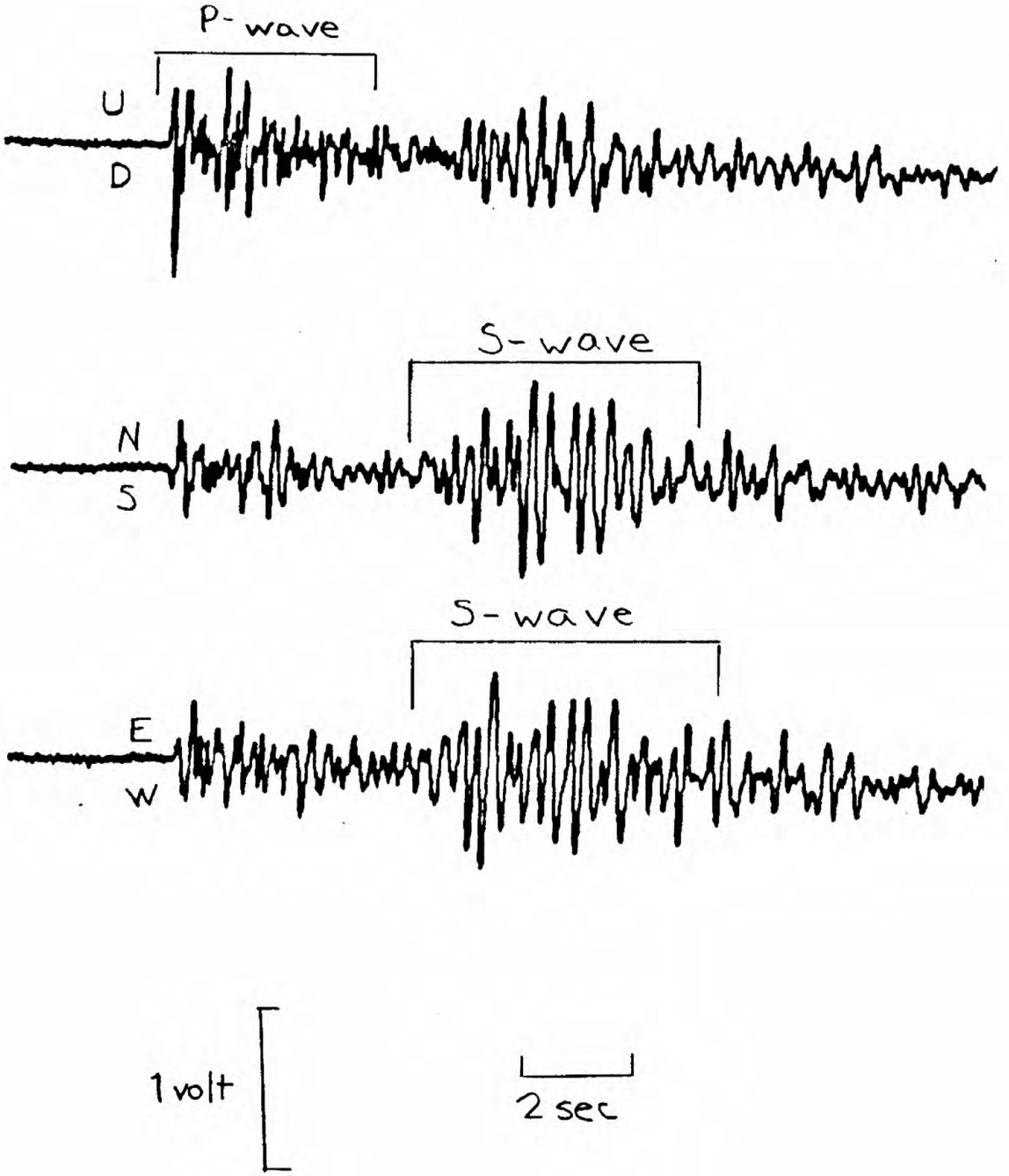

FIGURE 12. Vertical (top), north-south (middle), and east-west (bottom) components of motion recorded on the low-gain station at Quien Sabe Ranch (HQR) for the August 7, 1979, 05:56 (GCT) aftershock, $\Delta = 35$ km. Ordinate scale is the analog-tape output voltage (clipping level = $\pm$ 2 volts).

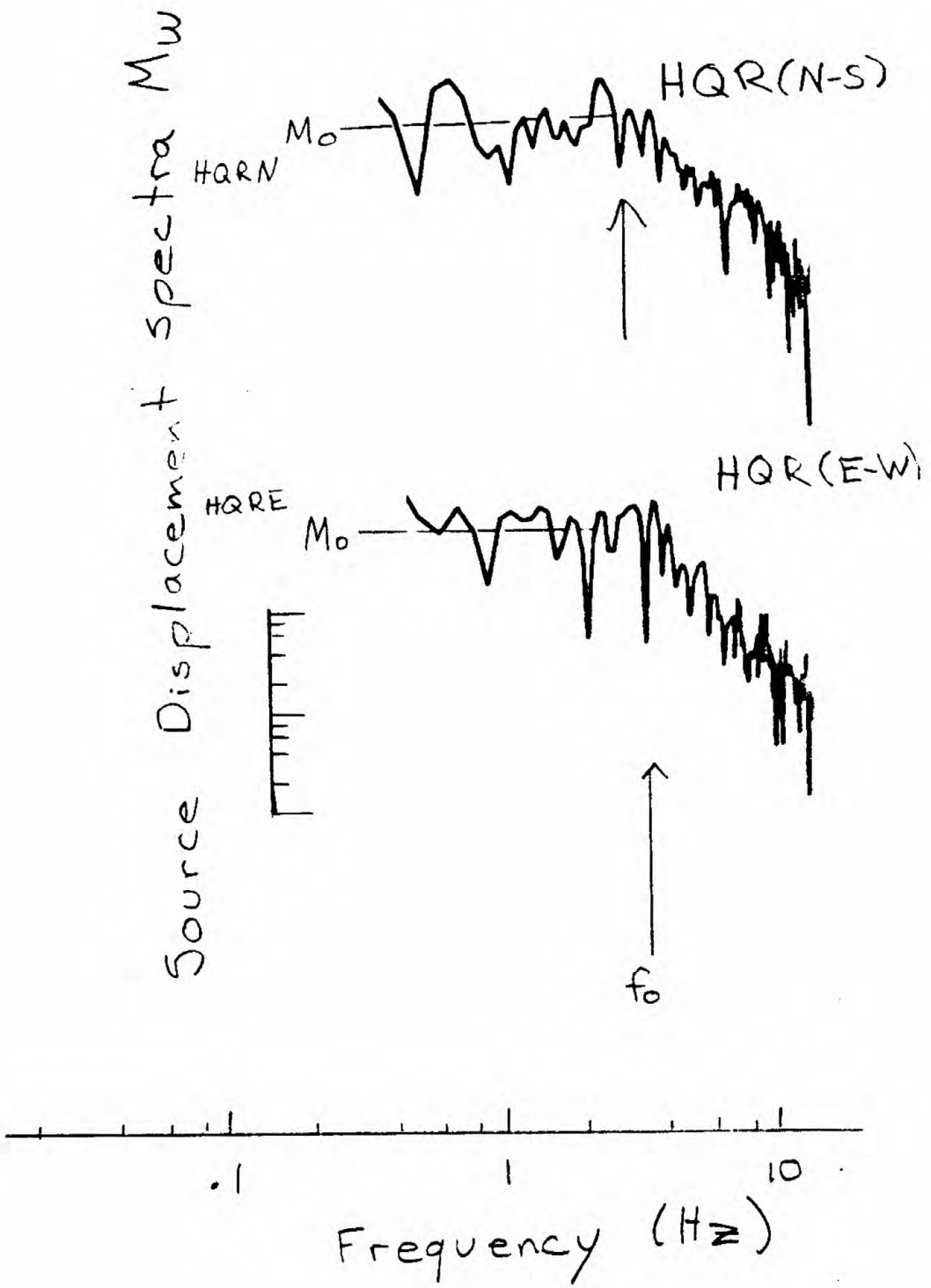

FIGURE 13. S-wave source-displacement spectra for the August 7, 1979, 05:56 (GCT) aftershock (see Fig. 12) recorded at Quien Sabe Ranch (HQR). M_o is the seismic moment and f_o the corner frequency.

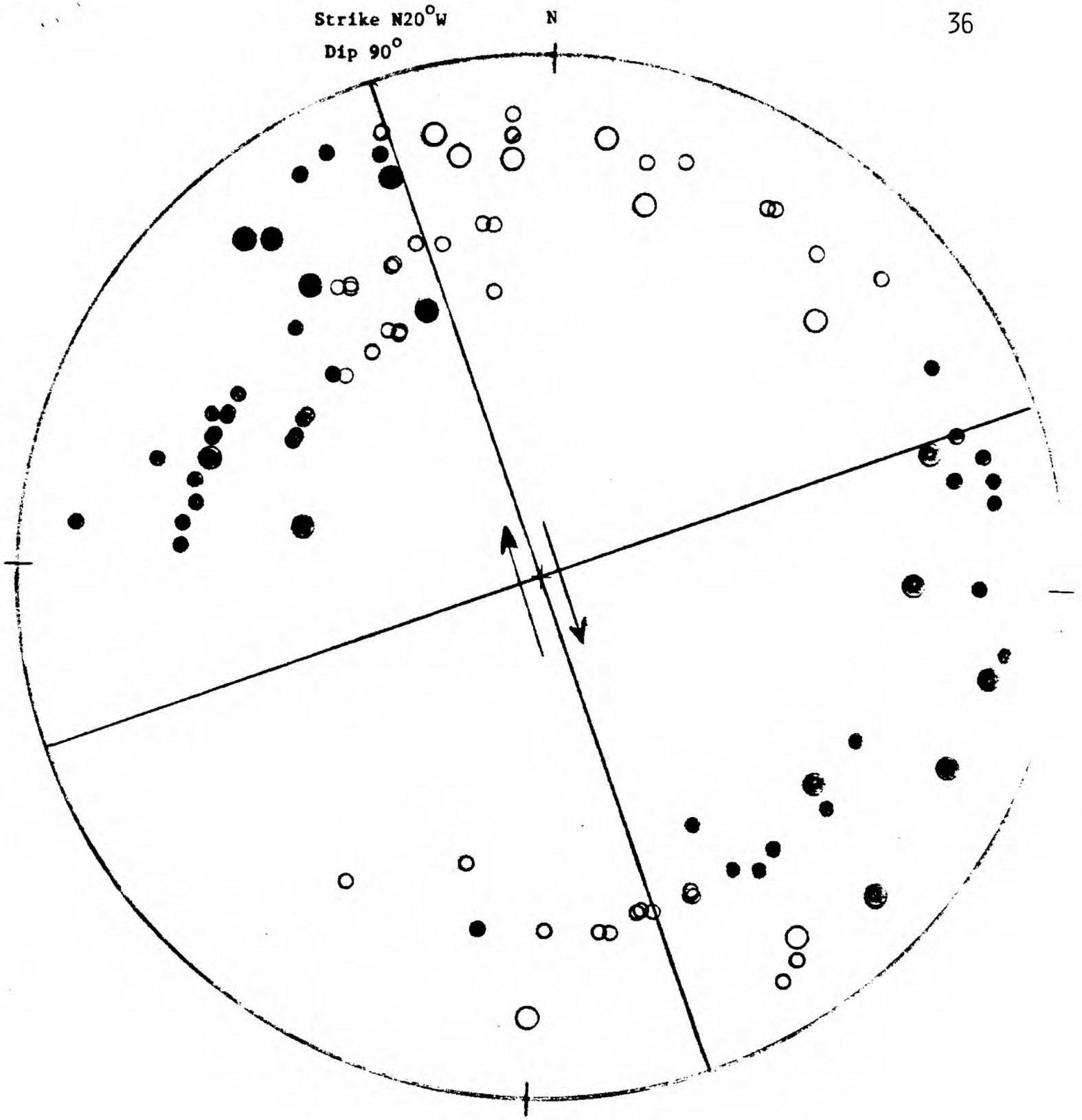

FIGURE 14. Nodal-plane solutions of the main shock based on first p-motion of 21 selected stations (large solid dots for compression and large open circles for dilatation). The diagram is an equal-area projection of the lower hemisphere. Small dots and small circles are first p-motion of stations not used in location and consequently not used for nodal-plane solution. They are plotted here to show that these additional data are by and large consistent with those used for location and nodal-plane solution.

TABLE 1. Station co-ordinates and corrections used in earthquake location.

STN	LAT	LONG	ELV(m)	DELAY(sec)
HGS	37°05.75'N	121°26.83'W	778	0.14
HPL	37°03.13'N	121°17.40'W	152	-0.08
HCA	37°01.52'N	121°29.02'W	332	0.07
HFE	36°59.00'N	121°24.09'W	323	-0.22
HLT	36°53.07'N	121°18.49'W	183	0.09
HQR	36°50.02'N	121°12.76'W	536	0.07
HCR	36°57.46'N	121°35.01'W	241	0.03
HOR	36°55.03'N	121°30.46'W	98	0.04
CAD	37°09.74'N	121°37.45'W	244	-0.26
CCO	37°15.46'N	121°40.35'W	366	0.20
CSC	37°17.11'N	121°46.35'W	128	0.07
HGW	37°01.02'N	121°39.02'W	133	-0.06
JAL	37°09.50'N	121°50.82'W	244	-0.13
JCB	37°06.71'N	121°41.33'W	192	0.0
JRR	37°03.27'N	121°43.61'W	408	-0.17
JST	37°12.41'N	121°47.84'W	149	-0.06
CAO	37°20.96'N	121°31.96'W	628	0.06
BVY	36°44.96'N	121°24.80'W	585	0.18
HFH	36°53.29'N	121°28.13'W	101	-0.04
HJG	36°47.88'N	121°34.43'W	171	0.24
HKR	36°54.10'N	121°25.56'W	66	-0.05

TABLE 2. List of Coyote Lake earthquake and its major aftershocks.

YEAR	MON	DY	HR	MN	SEC	LAT N	LONG W	DEPTH	MAG	NO	GAP	DMIN	RMS	ERH	ERZ	Q
1979	AUG															
		6	17	5	22.3	37- 6.7	121-32.0	9.6	5.7	21	102	7.8	0.11	0.4	1.1	B
		6	17	16	54.2	37- 3.4	121-30.2	6.9	1.1	10	106	3.9	0.05	0.3	0.7	B
		6	17	17	55.0	36-58.2	121-28.4	10.7	1.1	9	130	6.2	0.10	0.9	1.2	B
		6	17	18	49.1	36-59.4	121-27.6	9.8	1.4	10	110	5.3	0.10	0.8	1.0	B
		6	17	21	19.6	37- 3.5	121-30.3	7.8	1.8	12	55	4.1	0.06	0.3	0.7	A
		6	17	22	47.1	37- 2.8	121-29.4	11.1	3.5	15	53	2.4	0.06	0.3	0.3	A
		6	17	25	17.3	37- 3.4	121-30.0	11.1	1.3	12	53	3.7	0.08	0.5	0.5	A
		6	17	27	46.5	37- 5.0	121-31.1	7.0	1.7	12	81	6.4	0.06	0.3	0.7	A
		6	17	29	9.1	37- 3.9	121-30.7	2.2	1.6	11	62	5.0	0.16	0.8	1.4	B
		6	17	29	58.4	37- 3.8	121-30.1	10.1	1.6	14	59	4.5	0.06	0.3	0.4	A
		6	17	35	12.7	37- 3.4	121-30.5	6.6	0.9	5	121	4.2	0.01	0.1	0.2	C
		6	17	35	44.6	37- 3.6	121-30.2	9.9	1.6	13	69	4.1	0.09	0.5	0.6	A
		6	17	40	51.3	37- 4.4	121-32.9	0.8	1.0	8	103	7.9	0.13	1.1	0.9	B
		6	18	3	21.2	37- 3.1	121-30.6	7.4	1.8	13	52	3.8	0.04	0.2	0.5	A
		6	18	15	56.1	37- 4.4	121-30.8	7.6	1.7	14	71	6.0	0.06	0.3	0.6	A
		6	18	17	45.1	37- 2.6	121-29.5	10.5	2.5	15	53	2.0	0.06	0.3	0.3	A
		6	18	21	10.6	37- 3.5	121-30.2	6.0	2.1	14	55	4.1	0.09	0.4	0.9	A
		6	19	19	26.4	37- 3.6	121-29.9	9.1	2.0	15	54	4.0	0.08	0.4	0.6	A
		6	20	11	54.8	37- 3.6	121-30.1	10.3	1.9	15	56	4.3	0.06	0.3	0.3	A
		6	21	10	21.9	37- 3.0	121-30.8	7.9	1.6	12	53	3.9	0.08	0.4	0.9	A
		6	21	25	24.4	37- 2.5	121-29.6	10.1	1.9	14	52	2.0	0.05	0.3	0.2	A
		6	22	21	1.3	37- 2.4	121-29.4	9.3	3.6	17	54	1.7	0.09	0.4	0.5	A
		6	22	33	34.9	37- 1.9	121-30.0	8.8	1.4	12	62	1.6	0.05	0.3	0.5	A
		6	22	33	55.1	37- 0.5	121-29.8	5.8	4.0	18	43	2.2	0.11	0.4	0.8	A
		6	22	35	56.9	37- 0.3	121-29.6	7.8	3.7	14	91	2.4	0.12	0.5	0.8	B
		6	23	25	27.4	37- 4.9	121-30.9	10.3	1.9	14	78	6.3	0.05	0.2	0.3	A
		6	23	34	8.6	37- 0.4	121-29.9	5.3	1.9	17	43	2.3	0.08	0.3	0.6	A
		6	23	36	0.1	37- 2.1	121-30.0	9.6	3.1	17	49	1.9	0.08	0.3	0.4	A
		6	23	48	50.3	37- 1.8	121-29.9	9.6	2.0	15	63	1.4	0.06	0.3	0.4	A
		7	1	55	12.8	37- 2.3	121-30.1	9.4	2.3	15	51	2.2	0.05	0.3	0.4	A
		7	2	32	31.1	36-58.9	121-28.7	9.4	3.4	18	64	4.9	0.08	0.3	0.5	A
		7	2	51	10.9	36-58.8	121-29.0	8.6	1.8	16	63	5.1	0.09	0.4	0.5	A
		7	4	38	43.1	37- 4.9	121-30.6	10.6	1.9	14	78	6.2	0.08	0.4	0.4	A
		7	4	44	29.0	37- 5.9	121-32.6	4.3	2.0	13	89	8.5	0.14	0.6	1.0	B
		7	5	12	37.3	37- 0.6	121-28.8	9.5	1.9	17	57	1.7	0.07	0.3	0.3	A
		7	5	25	56.7	37- 1.1	121-30.3	5.4	2.0	17	43	2.0	0.05	0.2	0.3	A
		7	5	56	51.2	37- 3.8	121-30.3	8.8	3.2	14	59	4.5	0.08	0.4	0.6	A
		7	6	0	20.9	36-59.1	121-29.3	7.9	1.9	17	58	4.5	0.08	0.3	0.7	A
		7	6	23	47.7	37- 3.6	121-30.1	10.0	1.7	14	56	4.2	0.05	0.2	0.3	A
		7	6	37	46.7	37- 3.1	121-30.0	7.4	1.9	14	49	3.3	0.05	0.2	0.5	A
		7	6	59	51.4	37- 3.6	121-30.4	6.9	2.0	12	57	4.3	0.07	0.4	0.8	A
		7	7	5	4.6	37- 0.1	121-29.8	7.0	1.5	15	80	2.9	0.04	0.2	0.4	A
		7	7	31	9.6	36-58.9	121-29.2	8.3	2.9	17	60	4.8	0.08	0.3	0.6	A
		7	7	45	1.4	37- 3.5	121-30.3	10.1	1.7	14	55	4.1	0.07	0.3	0.4	A

YEAR	MON	DY	HR	MN	SEC	LAT N	LONG W	DEPTH	MAG	NO	GAP	DMIN	RMS	ERH	ERZ	Q
1979	AUG	7	8	11	36.4	37- 2.0	121-30.6	4.2	1.3	13	59	2.5	0.06	0.3	0.5	A
		7	9	8	7.6	37- 6.8	121-33.7	4.2	1.4	13	95	10.4	0.13	0.6	1.0	B
		7	9	9	21.1	37- 4.4	121-30.4	10.2	1.4	13	69	5.7	0.06	0.3	0.5	A
		7	13	21	30.0	37- 4.3	121-31.8	1.3	1.5	11	71	6.7	0.06	0.5	0.5	B
		7	13	47	37.5	37- 1.6	121-29.1	9.9	1.7	13	57	0.2	0.06	0.3	0.3	A
		7	13	59	16.1	37- 6.7	121-33.2	4.9	1.7	13	97	9.5	0.18	0.8	1.3	B
		7	14	15	33.3	37- 1.0	121-29.6	9.7	2.4	14	72	1.2	0.07	0.4	0.4	A
		7	14	57	50.9	37- 6.6	121-33.3	4.8	2.5	17	95	9.7	0.12	0.5	0.5	B
		7	18	31	12.0	37- 6.8	121-33.7	4.3	2.5	13	95	10.3	0.11	0.5	0.8	B
		7	18	51	46.3	36-59.5	121-29.3	6.7	2.6	17	55	3.8	0.10	0.4	1.0	A
		7	19	1	41.0	36-58.6	121-29.1	8.7	2.7	17	63	5.3	0.10	0.4	0.5	A
		7	19	11	25.3	36-59.2	121-28.9	8.7	3.4	17	59	4.3	0.13	0.6	0.7	A
		7	19	34	18.7	36-59.3	121-29.4	6.0	2.2	17	50	4.1	0.10	0.4	0.8	A
		7	19	58	50.6	36-58.6	121-29.3	7.9	2.1	15	61	5.4	0.10	0.4	0.8	A
		7	23	14	34.7	37- 0.5	121-29.8	6.9	2.1	16	61	2.2	0.07	0.3	0.6	A
		8	1	55	31.1	37- 1.1	121-30.2	5.3	2.2	17	43	1.9	0.08	0.3	0.6	A
		8	1	57	42.8	37- 0.3	121-28.2	11.6	2.4	17	61	2.6	0.07	0.3	0.2	A
		8	3	52	14.1	36-59.8	121-29.6	8.4	3.0	17	51	3.4	0.07	0.3	0.4	A
		8	8	3	47.9	37- 0.3	121-29.8	7.0	2.2	16	50	2.5	0.08	0.3	0.7	A
		8	8	6	25.1	37- 0.3	121-29.6	7.5	2.1	19	51	2.4	0.08	0.3	0.5	A
		8	12	29	58.4	36-59.5	121-29.8	7.9	2.2	19	49	3.9	0.09	0.3	0.5	A
		8	13	16	30.9	37- 1.6	121-29.4	8.8	2.1	19	55	0.5	0.05	0.2	0.4	A
		8	14	27	49.7	37- 3.6	121-31.2	6.4	2.3	12	60	5.0	0.07	0.4	0.9	A
		8	16	15	49.3	36-58.9	121-27.7	10.8	2.4	16	97	5.3	0.11	0.5	0.5	B
		8	17	34	17.1	37- 0.1	121-29.2	9.2	2.5	16	68	2.7	0.07	0.3	0.3	A
		8	22	56	7.5	37- 2.3	121-29.4	9.5	3.5	16	54	1.6	0.07	0.3	0.3	A
		9	1	28	2.5	37- 2.1	121-29.7	11.4	2.1	17	51	1.5	0.07	0.3	0.2	A
		9	4	47	35.5	37- 1.7	121-30.0	10.6	2.1	14	63	1.5	0.05	0.3	0.3	A
		9	5	28	48.2	36-58.8	121-29.0	9.1	3.2	17	63	5.1	0.08	0.3	0.4	A
		9	7	3	19.9	37- 1.5	121-26.7	9.4	3.9	17	60	0.4	0.09	0.4	0.4	A
		9	12	49	11.4	36-58.6	121-29.3	8.6	1.8	16	61	5.5	0.10	0.4	0.5	A
		9	12	49	27.3	36-58.4	121-28.9	6.5	3.5	17	66	5.7	0.12	0.5	1.2	A
		9	12	51	41.1	36-58.4	121-29.3	8.8	3.2	16	63	5.9	0.09	0.4	0.4	A
		9	12	54	17.2	36-58.6	121-29.1	7.6	2.3	16	60	5.4	0.10	0.4	0.6	A
		9	15	8	1.8	37- 1.1	121-30.1	6.4	2.3	16	42	1.8	0.06	0.2	0.5	A
		9	16	10	8.3	37- 0.1	121-27.6	11.5	2.1	16	63	3.4	0.07	0.4	0.3	A
		9	19	0	43.7	37- 7.5	121-32.8	4.7	2.1	8	134	18.4	0.09	0.6	0.7	B
		9	22	22	56.7	37- 2.1	121-30.2	6.2	2.7	16	48	2.1	0.06	0.2	0.5	A
		10	0	25	20.5	37- 1.6	121-29.0	9.3	3.7	14	72	0.2	0.08	0.4	0.4	A
		10	4	50	39.4	36-58.4	121-28.8	9.0	3.3	17	67	5.8	0.09	0.4	0.5	A
		10	5	10	42.3	36-58.3	121-28.5	9.1	3.2	16	72	6.1	0.11	0.5	0.7	A
		10	5	34	41.7	36-58.3	121-29.1	8.5	2.5	16	62	6.0	0.10	0.4	0.4	A
		10	5	53	5.7	36-58.4	121-28.6	8.8	2.5	18	69	5.8	0.11	0.4	0.6	A
		10	6	17	42.2	36-58.3	121-29.1	8.5	2.2	15	61	5.9	0.09	0.4	0.5	A
		10	7	51	54.8	36-56.5	121-28.2	8.9	2.2	19	65	4.3	0.17	0.6	0.9	B

YEAR	MON	DY	HR	MN	SEC	LAT N	LONG W	DEPTH	MAG	NO	GAP	DMIN	RMS	ERH	ERZ	Q
1979	AUG	10	7	53	25.4	36-59.2	121-26.7	11.6	2.2	19	63	3.9	0.12	0.5	0.4	A
		10	11	25	3.5	37- 8.9	121-33.3	8.0	2.1	19	109	11.3	0.10	0.3	1.5	B
		10	12	36	59.6	36-58.3	121-28.8	9.4	3.0	18	57	6.0	0.11	0.4	0.5	A
		10	12	38	54.6	36-58.2	121-28.9	9.4	2.1	19	58	6.1	0.11	0.4	0.5	A
		10	19	22	26.7	36-58.4	121-28.8	9.1	3.1	17	68	5.8	0.12	0.5	0.7	A
		10	20	36	17.2	36-58.2	121-28.9	8.9	2.0	15	80	6.2	0.12	0.5	0.6	A
		10	21	45	37.1	36-58.3	121-28.7	9.1	2.4	16	96	6.0	0.12	0.6	0.6	B
		11	3	58	56.9	37- 0.0	121-29.4	9.2	2.5	14	99	2.8	0.05	0.2	0.3	B
		11	9	40	19.0	36-59.5	121-29.0	9.5	3.3	16	98	3.7	0.07	0.3	0.4	B
		11	12	38	12.2	37- 1.3	121-29.1	8.9	2.0	16	57	0.4	0.07	0.3	0.6	A
		11	16	42	32.1	36-58.8	121-29.2	8.1	3.1	14	100	5.0	0.09	0.3	0.7	B
		11	19	50	32.1	36-57.7	121-28.9	8.4	2.7	17	62	5.4	0.14	0.5	0.6	A
		12	6	52	31.3	37- 0.3	121-29.6	8.5	2.7	17	51	2.5	0.08	0.3	0.5	A
		13	5	3	42.2	37- 7.1	121-32.6	3.8	1.6	18	104	9.0	0.10	0.6	1.1	B
		13	11	42	30.9	37- 2.0	121-29.1	10.0	1.6	17	57	1.0	0.07	0.3	0.3	A
		13	18	35	49.8	37- 4.6	121-31.9	5.0	2.4	16	106	7.1	0.09	0.4	1.2	B
		13	19	9	57.6	37- 4.3	121-32.5	4.0	2.2	15	101	7.3	0.15	0.6	1.0	B
		14	2	47	20.0	36-59.8	121-29.3	8.7	2.6	19	52	3.2	0.09	0.3	0.6	A
		14	3	15	56.7	36-59.6	121-29.4	9.1	3.9	19	52	3.5	0.09	0.3	0.4	A
		14	12	55	2.1	37- 3.1	121-30.3	7.1	2.2	18	51	3.5	0.06	0.2	0.5	A
		14	15	39	5.2	37- 8.8	121-33.3	5.7	2.4	19	109	11.1	0.09	0.3	1.8	B
		14	22	29	52.5	37- 2.1	121-30.4	7.2	2.4	19	46	2.4	0.08	0.3	0.5	A
		15	10	25	36.3	36-59.5	121-29.2	7.6	1.7	15	80	3.8	0.07	0.3	0.6	A
		15	17	52	32.9	37- 1.9	121-29.7	10.3	1.9	18	52	1.2	0.05	0.2	0.2	A
		15	23	5	29.9	37- 0.6	121-28.6	8.8	2.3	19	59	1.8	0.10	0.3	0.6	A
		16	5	39	16.7	37- 2.1	121-30.2	5.7	1.7	19	48	2.1	0.06	0.2	0.4	A
		16	10	10	1.7	36-59.8	121-29.6	8.1	2.0	19	51	3.4	0.08	0.3	0.5	A
		16	11	47	44.6	37-10.0	121-34.3	5.3	2.5	18	107	12.1	0.11	0.5	2.9	C
		16	11	59	58.0	36-59.2	121-29.1	9.3	2.2	19	52	4.3	0.07	0.2	0.3	A
		16	15	21	51.0	36-58.5	121-29.1	8.5	1.8	19	55	5.5	0.13	0.5	0.7	A
		16	22	24	41.2	36-58.3	121-28.3	9.4	1.8	16	53	6.1	0.12	0.5	0.7	A
		16	22	36	7.3	36-57.8	121-28.6	9.2	2.1	19	57	5.9	0.13	0.5	0.7	A
		17	2	43	29.1	37- 0.3	121-29.8	6.0	2.3	19	48	2.6	0.09	0.3	0.6	A
		17	2	53	54.3	36-59.4	121-29.3	8.4	2.3	19	51	3.9	0.07	0.3	0.4	A
		17	22	0	51.1	36-59.5	121-29.4	9.0	2.4	17	51	3.7	0.09	0.4	0.4	A
		18	9	30	51.4	37- 3.8	121-30.7	3.9	1.6	14	92	5.0	0.07	0.4	0.6	B
		18	9	38	4.5	37- 5.2	121-31.5	5.6	1.7	14	116	7.0	0.08	0.4	1.1	B
		18	21	42	7.1	37- 9.4	121-33.4	6.8	1.8	16	110	12.0	0.10	0.4	2.3	B
		18	21	55	57.4	37- 3.6	121-30.4	7.4	1.6	17	57	4.4	0.06	0.2	0.5	A
		19	2	6	55.4	37- 2.2	121-30.0	5.4	2.2	18	49	1.9	0.06	0.2	0.4	A
		19	4	42	2.8	37- 0.5	121-29.1	7.1	2.1	18	55	1.9	0.08	0.3	0.6	A
		19	8	45	50.1	36-58.4	121-29.1	7.5	2.6	20	57	5.8	0.11	0.4	0.7	A
		19	8	58	51.3	36-58.3	121-29.0	8.0	2.0	18	57	5.9	0.11	0.4	0.8	A
		19	17	58	25.9	37- 4.5	121-31.2	9.6	1.8	16	72	6.3	0.09	0.4	0.9	A
		19	20	31	37.2	37- 6.1	121-31.7	7.5	1.5	14	132	7.2	0.13	0.6	1.4	B

YEAR	MON	DY	HR	MN	SEC	LAT N	LONG W	DEPTH	MAG	NO	GAP	DMIN	RMS	ERH	ERZ	Q
1979	AUG	20	3	12	5.1	37- 1.6	121-30.1	4.4	1.7	17	63	1.6	0.10	0.4	0.5	A
		20	8	12	58.1	37- 1.7	121-29.9	6.2	1.7	15	85	1.4	0.04	0.2	0.4	A
		20	11	52	53.3	37- 1.6	121-30.1	5.1	2.0	18	49	1.7	0.07	0.3	0.6	A
		20	13	53	17.9	37- 2.3	121-29.4	11.2	2.5	17	54	1.6	0.09	0.4	0.3	A
		20	22	13	3.6	37- 7.3	121-32.5	3.8	1.5	12	107	8.9	0.05	0.3	0.5	B
		21	5	7	46.2	36-56.8	121-39.5	4.4	1.8	18	169	6.8	0.10	0.4	1.1	B
		21	5	30	55.5	36-59.1	121-27.5	12.0	1.8	19	59	5.0	0.08	0.4	0.4	A
		21	7	10	59.0	36-59.9	121-27.7	10.6	1.9	18	62	3.5	0.08	0.3	0.4	A
		21	8	22	58.1	36-59.4	121-29.1	9.0	1.7	19	52	4.0	0.09	0.3	0.4	A
		21	9	44	26.7	37- 5.0	121-31.2	7.4	1.7	18	80	6.6	0.07	0.3	0.6	A

TABLE 3. Source parameters for some Coyote Lake aftershocks.

DATE	TIME h m s	SEISMIC MOMENT (dyne-cm)	SOURCE RADIUS (km)	STRESS DROP (bars)
790806	171654	$(1.71 \pm 0.36) \times 10^{18}$		
	171755	$(1.70 \pm 0.38) \times 10^{18}$		
	173153	$(3.80 \pm 1.07) \times 10^{17}$		
	173512	$(6.00 \pm 1.76) \times 10^{17}$		
	174051	$(7.00 \pm 0.86) \times 10^{17}$		
	222101	$(8.99 \pm 1.49) \times 10^{20}$	0.43	4.2
	223355	$(5.77 \pm 1.22) \times 10^{21}$		
790807	015513	$(2.93 \pm 0.67) \times 10^{19}$		
	023231	$(2.99 \pm 0.36) \times 10^{20}$	0.65	0.5
	051237	$(1.21 \pm 0.17) \times 10^{19}$		
	052556	$(9.13 \pm 1.47) \times 10^{18}$		
	055651	$(2.56 \pm 0.41) \times 10^{20}$	0.43	1.4
	062347	$(5.61 \pm 1.03) \times 10^{18}$		
	070504	$(5.50 \pm 1.09) \times 10^{18}$		
	073109	$(7.04 \pm 1.02) \times 10^{19}$	0.33	0.9
	090921	$(2.80 \pm 0.41) \times 10^{18}$		
	141533	$(4.77 \pm 0.76) \times 10^{19}$		
790809	124927	$(8.40 \pm 0.93) \times 10^{20}$		
790810	002520	$(1.25 \pm 0.19) \times 10^{21}$		
790818	093051	$(2.78 \pm 0.46) \times 10^{18}$		
790819	020655	$(2.00 \pm 0.31) \times 10^{19}$		
	044202	$(8.03 \pm 1.12) \times 10^{18}$		